НАУЧНАЯ СТАТЬЯ SCIENTIFIC ARTICLE
УДК 625.731.8 UDC 625.731.8
https://doi.org/10.56195/20793332-2025-25-6-32-39

# Failure mechanism and stability control of roadways under challenging geological conditions

**L. Lu**[1,2]✉
[1] *China University of Mining and Technology-Beijing, China*
[2] *China-Russia Dynamics Research Center, China University of Mining and Technology-Beijing, China*
✉ *linlu_cumtb@163.com*

***Abstract.*** In special geological zones formed by coal seam spontaneous combustion, burnt rock exhibits a loose structure, well-developed joints and fissures, and significantly reduced strength, resulting in considerable challenges for roadway stability control. This paper investigates the deformation and failure characteristics and stability control mechanisms of roadway surrounding rock affected by thermal alteration, using the 3202 return airway of Dawan Coal Mine as a case study. Based on the Hoek-Brown strength criterion and elastic-plastic mechanics theory, a stability analysis model for burnt rock roadway surrounding rock was established. The extent of the loosening zone was verified through UDEC numerical simulation and borehole observations, revealing a loosening zone depth ranging from approximately 3.1 m to 4.2 m. To address these challenges, this paper proposes a comprehensive control technology based on multi-stage coordinated support, termed the Reinforcement-Anchorage-Constraint (RAC) system. This system integrates grouting reinforcement (Reinforcement), bolt and cable support (Anchorage), and metal shed support (Constraint) to ensure roadway stability. Field monitoring results demonstrate that the roof-to-floor convergence is 71 mm and the ribs convergence is 27 mm, indicating overall roadway stability. The research findings provide both theoretical foundation and practical engineering guidance for stability control of roadways in burnt rock zones.

***Keywords:*** Burnt rock, Roadway stability, Hoek-Brown criterion, Combined support system, Field test

***For citation:*** Lu L. Failure mechanism and stability control of roadways under challenging geological conditions. *Mine Surveying and Subsurface Use*. 2025;25(6):32-39. https://doi.org/10.56195/20793332-2025-25-6-32-39.

# Механизм разрушения и контроль устойчивости автомобильных дорог в сложных геологических условиях

**Л. Лу**[1,2]✉
[1] *Китайский университет горного дела и технологий – Пекин, Китай*
[2] *Центр исследований динамики взаимоотношений между Китаем и Россией, Китайский университет горного дела и технологий – Пекин, Китай*
✉ *linlu_cumtb@163.com*

***Резюме.*** В особых геологических зонах, образованных самовозгоранием угольных пластов, горелая порода имеет рыхлую структуру, хорошо развитые соединения и трещины, а также значительно сниженную прочность, что приводит к значительным проблемам контроля устойчивости выработки. В данной статье исследуются характеристики деформации и разрушения, а также механизмы контроля устойчивости породы вокруг выработки, пострадавшей от термических изменений, на примере вытяжного воздуховода 3202 угольной шахты Давань. На основе критерия прочности Хука-Брауна и теории упругопластической механики была создана модель анализа устойчивости окружающей выработки из горелой породы. Протяженность зоны разрыхления была проверена с помощью численного моделирования UDEC и наблюдений за скважинами, выявивших глубину зоны разрыхления приблизительно от 3,1 м до 4,2 м. Для решения этих проблем в данной статье предлагается комплексная технология контроля, основанная на многоступенчатой скоординированной поддержке, называемая системой армирования-анкерования-ограничения (RAC). Эта система объединяет в себе армирование бетонной смесью (армирование), анкерное крепление болтами и тросами (анкерное крепление) и металлическую опору навеса (ограничение) для обеспечения устойчивости дорожного полотна. Результаты натурных наблюдений показывают, что схождение кровли и пола составляет 71 мм, а схождение ребер – 27 мм, что свидетельствует об общей устойчивости дорожного полотна. Результаты исследования предоставляют как

теоретическую основу, так и практические инженерные рекомендации по контролю устойчивости дорожного полотна в зонах горелых пород.

***Ключевые слова:*** горелая порода, устойчивость дорожного полотна, критерий Хука-Брауна, комбинированная система поддержки, полевые испытания

***Для цитирования****:* Лу Л. Механизм разрушения и контроль устойчивости автомобильных дорог в сложных геологических условиях. *Mine Surveying and Subsurface Use*. 2025;25(6):32-39. (In Russ.). https://doi.org/10.56195/20793332-2025-25-6-32-39.

## Introduction

Shallow coal seams are highly susceptible to spontaneous combustion due to surface weathering and oxidation conditions. Under high temperature heating and thermal effects, the surrounding rock structure and composition in coal seam spontaneous combustion zones undergo alterations and transform into burnt rock [1–3]. As a special rock type, burnt rock commonly exhibits characteristics such as loose structure, well-developed joints and fissures, and high porosity. Its overall mechanical properties are significantly deteriorated, leading to reduced bearing capacity of the surrounding rock and thereby posing severe challenges to the stability control of underground roadways.

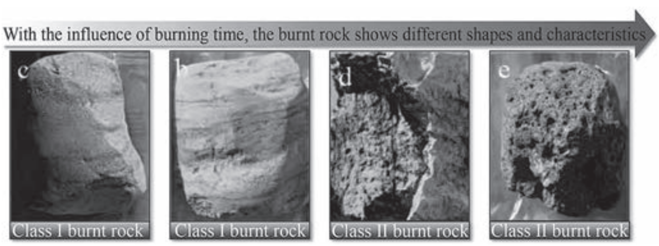


***Fig. 1.*** **Characteristics of burnt rock [1]**

Currently, China's coal resource mining intensity continues to increase, with massive underground roadway engineering scale, and the length of newly excavated roadways exceeds 12,000 km annually [4–7]. Conventional support designs frequently fail in burnt rock areas, easily triggering safety hazards such as surrounding rock instability, collapse, and excessive deformation, causing serious safety risks and economic losses.

Existing research has achieved significant progress in disaster prevention and safe mining in burnt coal seam areas, primarily focusing on hydraulic connectivity, structural characteristics, and boundary identification of burnt zones [8–11]. However, research on the stability mechanisms of surrounding rock during roadway excavation in burnt rock and corresponding control technologies remains relatively limited.

This study takes the 3202 return airway of Dawan Coal Mine as a case study to analyze the factors influencing roadway stability in burnt rock zones and the failure mechanisms of surrounding rock, determine the extent of the loosening zone, and propose a comprehensive control technology termed the Reinforcement-Anchorage-Constraint (RAC) system The effectiveness of this approach has been validated through field application.

## Engineering background and failure observations

This study focuses on the 3202 working face roadway of Dawan Coal Mine in the Shenfu mining area, Yulin City, Shaanxi Province. The mine currently extracts the 3-1 coal seam at a depth of approximately 150 m, with an average thickness of 3.1 m and a simple seam structure. The strata attitude trends high in the northeast and low in the southwest, with an average dip angle of 0.5°.

The coal seam overlying the 3202 return airway has been completely oxidized and eroded. The eastern and northern portions of the 3-1 coal seam are located within the burnt zone, causing localized areas of the 3202 working face to be affected by thermal effects from the burnt region, as shown in ***Fig. 2***(a). The lithology of the working face roof and floor is presented in ***Fig. 2***(b). Due to the influence of the burnt zone, substantial smoke emissions and surface cracks are observed at the mine surface, as shown in ***Fig. 2***(c).

The 3202 return airway has a rectangular cross-section with dimensions of 5500 mm (width) × 3000 mm (height). The initial support scheme employed bolt-mesh-cable support. The roadway roof and non-mining rib utilize Φ20 mm × 2000 mm left-handed thread steel bolts, while the mining rib employs Φ18 mm × 1800 mm fully-threaded resin bolts, both with a spacing of 1000 mm × 1000 mm. The bolts are end-anchored using CK2360 resin cartridges. One Φ15.24 mm × 6300 mm steel strand cable is installed at the roof center with a row spacing of 3000 mm, as illustrated in ***Fig. 2***(d).

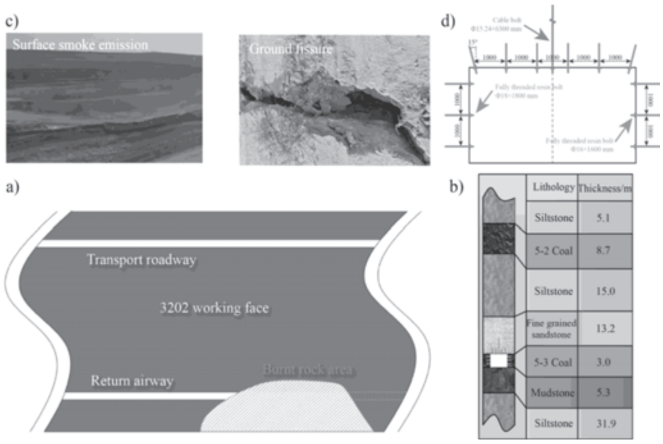


***Fig. 2.*** **Comprehensive geological column and working face layout**

During roadway excavation, the surrounding rock experiences degradation of its structure and mechanical properties due to prolonged exposure to high temperatures from the adjacent burnt rock, resulting in significantly reduced overall integrity and stability.

At the excavation face, it can be observed that the roof is affected by the burnt zone, with color changes appearing yellow and brown, and a large number of cracks and separations appearing. Field investigations (***Fig. 3***) reveal the following main problems: (1) The roof structure is loose with poor integrity; (2) The surrounding rock strength is reduced with insufficient bearing capacity; (3) The existing support system is difficult to adapt to the deformation characteristics of burnt rock surrounding rock.

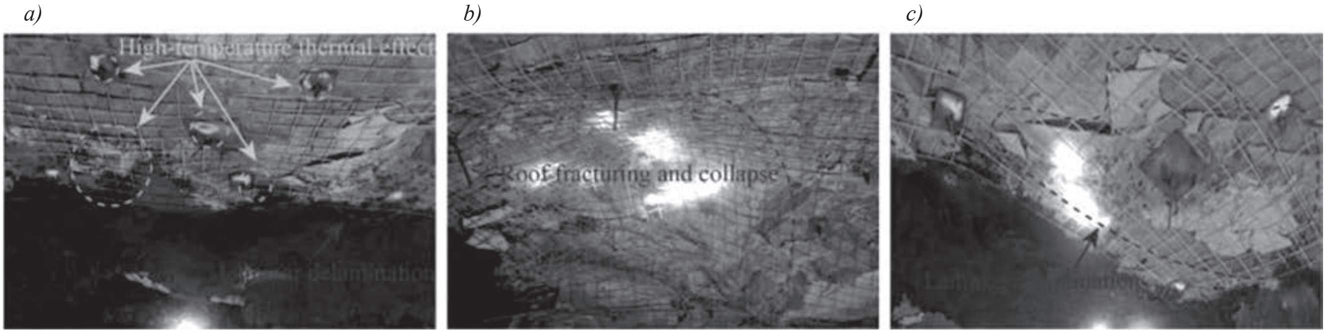


***Fig. 3.*** **Deformation and failure of roadway surrounding rock**

**Roadway Stability Analysis in Burnt Rock Zones**

To deeply analyze the stability of roadway surrounding rock in burnt rock zones, this paper adopts the Hoek-Brown strength criterion to theoretically calculate the range of the plastic zone of surrounding rock. By introducing the Hoek-Brown constant $m_1$, disturbance factor $\alpha$, rock mass fragmentation degree index $s$, and geological strength index GSI into the Hoek-Brown criterion, an accurate evaluation of roadway stability in areas affected by burning alteration is conducted.

The mechanical model of roadway surrounding rock zoning in burnt rock areas is shown in ***Fig. 4***. The roadway surrounding rock is divided into three zones: the elastic zone, plastic softening zone, and fractured zone.

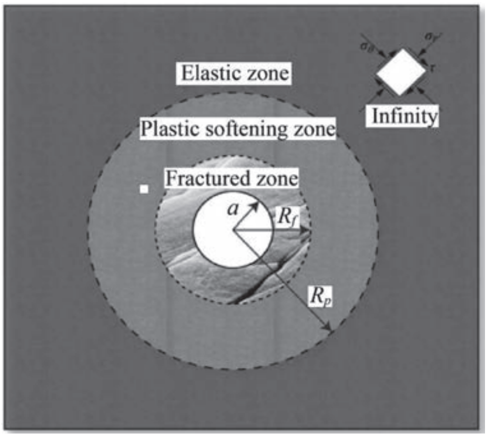


***Fig. 4.*** **Roadway mechanical model**

Based on the above assumptions, the problem can be simplified to an axisymmetric plane strain problem. The equilibrium differential equation in polar coordinates can be expressed as:

$$\frac{d\sigma_r}{dr}+\frac{\sigma_r-\sigma_\theta}{r}=0 \tag{1}$$

When plastic yielding and fracturing occur in the roadway surrounding rock, the stress conditions satisfy the modified Hoek-Brown failure criterion, which can be expressed as:

$$\begin{aligned}&\sigma_\theta=\sigma_r+\sigma_c\cdot\left(m\cdot\frac{\sigma_r}{\sigma_c}\cdot e^{\frac{GSI-100}{28}}+s\right)^{\alpha}\\&m=m_i\cdot e^{\frac{GSI-100}{28}}\\&s=e^{\frac{GSI-100}{9}}\end{aligned} \tag{2}$$

where: $\sigma_\theta$ is the tangential stress at any point; $\sigma_r$ is the radial stress at any point; $\sigma_c$ is the uniaxial compressive strength of rock; $m_1$ and $\alpha$ are dimensionless empirical parameters for different rock masses; $s$ is the rock mass fragmentation degree index, with a value range of 0.0~1.0; $GSI$ is the geological strength index of rock mass.

According to elastoplastic mechanics, the stress distribution in the elastic zone is:

$$\begin{cases}\sigma_r^e=P_0\left(1-\dfrac{R_e^2}{r^2}\right)+\sigma_{r|r=R_e}\dfrac{R_e^2}{r^2}\\ \sigma_\theta^e=P_0\left(1+\dfrac{R_e^2}{r^2}\right)-\sigma_{r|r=R_e}\dfrac{R_e^2}{r^2}\end{cases} \tag{3}$$

By simultaneously solving the equilibrium equation and the modified H-B failure criterion subject to the stress and displacement boundary conditions of the plastic softening zone, the stress distribution is expressed as:

$$\begin{aligned}\sigma_r^p&=\frac{\sigma_c}{m_r^p}\left[m_r^p(1-\alpha)\ln\left(\frac{r}{R_p}\right)+\left(m_r^p\frac{\sigma_{r|r=R_f}}{\sigma_c}+s_r^p\right)^{1-\alpha}\right]^{\frac{1}{1-\alpha}}-\frac{\sigma_c}{m_r^p}s_r^p\\ \sigma_\theta^p&=\frac{\sigma_c}{m_r^p}\left[m_r^p(1-\alpha)\ln\left(\frac{r}{R_p}\right)+\left(m_r^p\frac{\sigma_{r|r=R_f}}{\sigma_c}+s_r^p\right)^{1-\alpha}\right]^{\frac{1}{1-\alpha}}-\frac{\sigma_c}{m_r^p}s_r^p\\ &+\sigma_c\left[m_r^p(1-\alpha)\ln\left(\frac{r}{R_p}\right)+\left(m_r^p\frac{\sigma_{r|r=R_f}}{\sigma_c}+s_r^p\right)^{1-\alpha}\right]^{\frac{\alpha}{1-\alpha}}\end{aligned} \tag{4}$$

where $m_r^p$, $s_r^p$, α are the Hoek-Brown parameters for the strain-softening rock mass; $\sigma_{r|r}=R_f$ is radial stress at the boundary of the plastic softening zone.

According to the stress boundary conditions of the roadway fractured zone and the H-B yield criterion, the stress distribution can be obtained as:

$$\begin{cases}\sigma_r^f=\dfrac{\sigma_c}{m_r^f}\left[m_r^f(1-\alpha)\ln\left(\dfrac{r}{a}\right)+\left(m_r^f\dfrac{P_i}{\sigma_c}+s_r^f\right)^{1-\alpha}\right]^{\frac{1}{1-\alpha}}-\dfrac{\sigma_c}{m_r^f}s_r^f\\ \sigma_\theta^f=\dfrac{\sigma_c}{m_r^f}\left[m_r^f(1-\alpha)\ln\left(\dfrac{r}{a}\right)+\left(m_r^f\dfrac{P_i}{\sigma_c}+s_r^f\right)^{1-\alpha}\right]^{\frac{1}{1-\alpha}}-\dfrac{\sigma_c}{m_r^f}s_r^f\\ \quad+\sigma_c\left[m_r^f(1-\alpha)\ln\left(\dfrac{r}{a}\right)+\left(m_r^f\dfrac{P_i}{\sigma_c}+s_r^f\right)^{1-\alpha}\right]^{\frac{\alpha}{1-\alpha}}\end{cases} \tag{5}$$

where $P_i$ is the support load.

$$\begin{cases} R_f = a\cdot\exp\left\{\dfrac{1}{m_f\sigma_c}\left[(\alpha-1)m_f\sigma_c+(1-\alpha)\left((m_f)^{\frac{1}{1-\alpha}}\sigma_c^{\frac{1}{1-\alpha}}+\dfrac{2\sigma_c\left(s_f\sigma_c+\dfrac{2P_0m_f}{1-\alpha}\right)}{1-\alpha}\right)^{1-\alpha}\right]-\dfrac{(s_f)^{1-\alpha}}{(1-\alpha)m_f}\right\} \\ R_p = R_f\cdot\exp\left\{\dfrac{1}{m_p\sigma_c}\left[(\alpha-1)m_p\sigma_c+(1-\alpha)\left((m_p)^{\frac{1}{1-\alpha}}(\sigma_c)^{\frac{1}{1-\alpha}}+\dfrac{2\sigma_c\left(s_p\sigma_c+\dfrac{2P_0m_p}{1-\alpha}\right)}{1-\alpha}\right)^{1-\alpha}\right]-\dfrac{\left(m_p\sigma_c\sigma_r^p+s_p\sigma_c^2\right)^{1-\alpha}}{(1-\alpha)\sigma_c m_p}\right\}-a \end{cases} \quad (6)$$

where $P_0$ is the in-situ stress.

Based on stress continuity at the elastic-plastic interface, the analytical solution for the radius of the roadway loosening zone is derived as:

After the rock mass is burnt, the rock mass exhibits reduced GSI and uniaxial compressive strength, while the effects of the Hoek-Brown parameter $m_1$ and rock mass integrity on stability become more pronounced. When exposed to groundwater, structural stability deteriorates significantly, with coal degrading to a mud-like state and *GSI* values predicted below 50[12]. Using parameters $m_1 = 8$, $GSI = 45$, $\sigma_c = 20$ MPa, and $P_0 = 3$ MPa, the calculated extent of the loosening zone surrounding the 3202 return airway reaches approximately 3.8 m.

### Validation of the Equivalent Radius Method

To validate the theoretical analysis presented above, UDEC numerical simulations were conducted to examine the extent of the plastic zone in the surrounding rock for both the equivalent circular and rectangular roadways. The plastic deformation characteristics are illustrated in ***Fig. 5***.

The simulation results demonstrate that the plastic zone depth of the equivalent circular model closely matches that of the rectangular roadway. For the equivalent circular roadway, the plastic failure depth in the roof reaches approximately 3.5 m, with a maximum depth of 2.9 m in the ribs. For the rectangular roadway, the roof plastic failure depth is approximately 3.7 m, with a maximum rib depth of about 3.0 m.

Comparison between the calculated and simulated results indicates that the theoretical model based on the equivalent radius method accurately captures the plastic zone distribution characteristics of roadway surrounding rock in burnt rock zones, thereby demonstrating the applicability of this method and validating the theoretical analysis.

To further validate the theoretical calculations and numerical simulation results, in-situ observations of the loosening zone extent in the 3202 return airway surrounding rock were conducted using a YTJ20 borehole observations system (Fig. 6). Boreholes were drilled at the left rib (1#), right rib (2#), and roof (3#), each with a depth of 8.0 m and diameter of 28 mm. The rib boreholes were oriented at 25° to the normal of the rib surface.

The observations reveal that the loosening zone in the roadway surrounding rock within the burnt rock area exhibits pronounced asymmetric distribution. The loosening zones in the left and right ribs extend approximately 3.1 m from the rib surface, while the roof loosening zone extends to 4.2 m. The extent of the loosening zone is in good agreement with both the theoretical calculations and UDEC numerical simulation results, confirming the reliability and applicability of the established theoretical model.

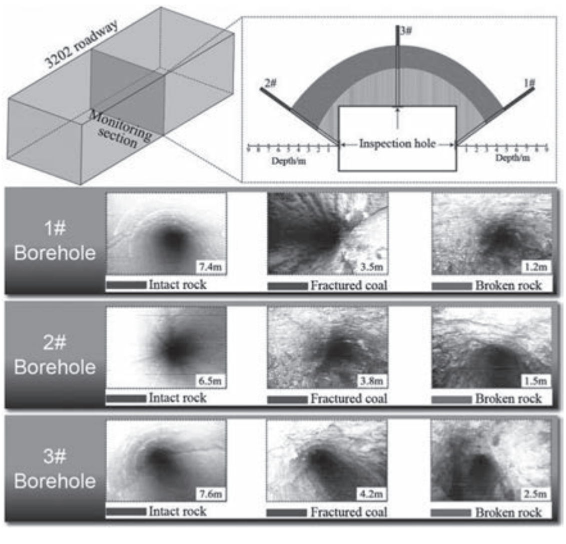


***Fig. 6.*** **Borehole observation layout and monitoring results**

*a)* *b)*

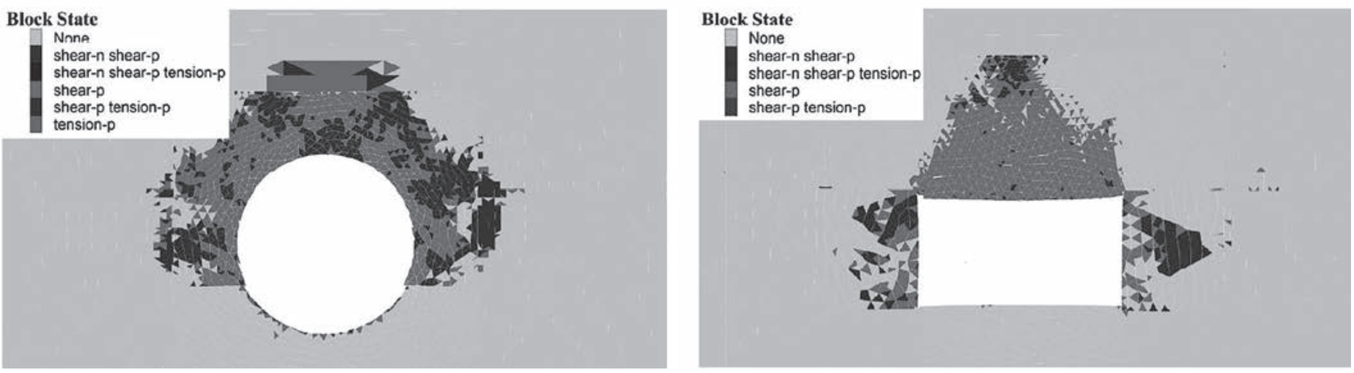


***Fig. 5.*** **Plastic failure zones in roadways: (a) Equivalent circular roadway; (b) Rectangular roadway**

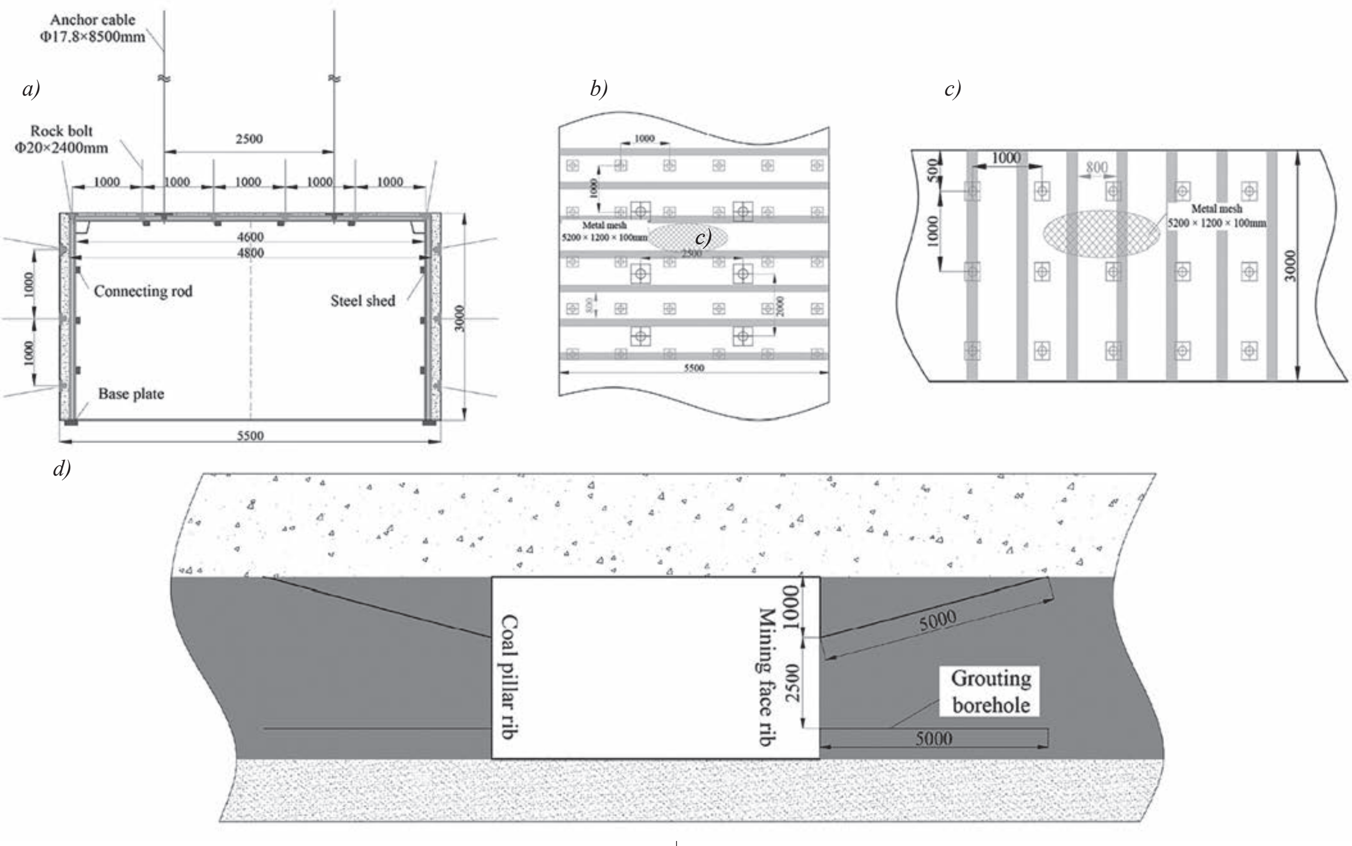


***Fig. 7.*** **Combined support of roadway: (a) Support section (b) Roof support (c) Rib support (d) Grouting borehole layout**

### Design of the RAC System

Based on the stability analysis of the roadway surrounding rock and the extent of the loosening zone in the burnt rock area, the RAC system was designed for the 3202 return airway at Dawan Coal Mine. The system integrates the three components of grouting reinforcement, bolt and cable support and metal shed support, as illustrated in ***Fig. 7***.

(1) Grouting reinforcement

The burnt rock area adopts Marissan-type polymer material for grouting reinforcement, with a grouting final pressure of 1-2 MPa and an effective diffusion radius of 1.5-2.0 m. Two types of grouting boreholes, designated as L and LX, are installed in the coal pillar rib and mining rib of the 3202 return airway. Type L boreholes are positioned 1.0 m below the roof with an upward inclination of 15° and a depth of 5.0 m, while type LX boreholes are located 2.5 m below the roof with a horizontal orientation and a depth of 5.0 m. Both borehole types are arranged in a single row with 5.0 m spacing.

(2) Rock bolt and cable support

The roof and solid coal rib are supported using Φ20 mm × 2400 mm fully threaded steel bolts, while the mining rib employs Φ22 mm × 2500 mm threaded steel resin bolts. All bolts are installed at a spacing of 1000 mm × 1000 mm and anchored with CK2360 resin cartridges. Additionally, two Φ17.8 mm × 8500 mm steel strand cables are installed symmetrically on either side of the roof centerline at a spacing of 2500 mm × 2000 mm.

(3) Metal shed support

Metal sheds are made of 11# mining I-beam steel, with an erection spacing of 800 mm. Adjacent metal sheds are connected by 7 round steel connecting rods, and the roof and both ribs are filled with semi-circular wooden backing plates.

### Interaction Characteristics between Support and Surrounding Rock

To investigate the mechanical response of roadway surrounding rock in burnt rock zones under different support systems, UDEC simulations were conducted for three support conditions: (1) unsupport, (2) bolt-cable support, and (3) RAC system. The analysis focused on stress distribution, deformation characteristics, and fracture development in the surrounding rock. The parameters used in the simulation were determined according to the engineering analogy method, and combined with mine grouting practice and related research [13–15]coal mine roadways under complex conditions were divided into five types, for each type the deformation and damage characteristics of rocks surrounding roadways were analyzed. The recent developments of roadway support technologies were introduced abroad, based on the experiences of supports for deep and complex roadways from Germany, the United States and Australia. The history and achievements of roadway support technologies in China were detailed, including rock bolting, steel supports, grouting reinforcement and combined supports. Four typical support and reinforcement case studies were analyzed, including a high stressed roadway 1,000 m below the surface, a roadway surrounded by severely weak and broken rocks, a chamber surrounded by weak and broken rocks, and a roadway with very soft and swelling rocks. Based on studies and practices in many years, rock bolting has become the mainstream roadway support form in China coal mines, and steel supports, grouting reinforcement and combined supports have also been applied at proper occasions, which have provided reliable technical measures for the safe and high effective construction and mining of underground coal mines.”,”container-title”:”International Journal of Coal Science & Technology”,”DOI”:”10.1007/

s40789-014-0043-0”,”ISSN”:”2095-8293, 2198-7823”,”issue”:”3”,”journalAbbreviation”:”Int J Coal Sci Technol”,”language”:”en”,”page”:”261-277”,”source”:”DOI.org (Crossref. The final selection was that after grouting, the rock mass cohesion increased by 20%, tensile strength increased by 5 kPa, and friction angle increased by 5°.

As shown in ***Fig. 8***, under unsupport conditions, the maximum principal stress zones in the roadway ribs and roof-to-floor extend deeply into the surrounding rock, forming pronounced stress concentrations. After applying rock bolt-cable support, the range of these concentrations decreases moderately, although local tensile stress zones persist. Combined support, integrating bolts, cables, metal sheds, and grouting, fills fractures and pores, enhances the integrity of the surrounding rock, and markedly reduces both the magnitude and extent of the principal stress concentrations.

The extent of tensile stress zones varies significantly under different support schemes, following the sequence: unsupport > bolt-cable support > RAC system. The corresponding peak tensile stresses are 1.14 MPa, 0.85 MPa, and 0.81 MPa, respectively. Compared with the unsupport and bolt-cable schemes, the RAC system reduces the maximum tensile stress by 29% and 5%, demonstrating a notable improvement in roadway stability.

Deviatoric stress is a critical factor governing plastic failure in the rock mass (***Fig. 9***). Under unsupport and bolt-cable support conditions, the deviatoric stress value in the shallow surface zone is relatively low (< 1.2 MPa), with high stress concentrated within the rib interior. In the unsupport case, peak deviatoric stress occurs at a distance of 2.59 m from the rib surface, whereas bolt-cable support causes this peak to migrate inward to 1.44 m from the rib. Under the RAC system, the deviatoric stress distribution shows an asymmetric form, with the maximum value concentrated at 0.83 m from the roadway floor corner, and the stress peak value is about 3.7 MPa. The failure range of shallow rock mass is significantly reduced, and roadway stability is obviously improved.

As shown in ***Fig. 10*** under unsupport conditions, the roof suffers from severe separation and inverted V-shaped failure due to tensile stress. Bolt-cable support restricts fracture propagation and interlayer sliding to a certain extent, but potential shear fractures still exist. The RAC system scheme significantly inhibits fracture development in the roof and ribs, roof displacement is obviously reduced, and the separation phenomenon is basically eliminated.

The axial force distribution in support components under different support schemes is illustrated in ***Fig. 11***. Under bolt-cable support, the mean axial force in bolts is 33.5 kN, approximately 28% of the breaking load, while the mean axial force in cables is 49 kN, approximately 18% of the breaking load, indicating low utilization. Under RAC system, the mean bolt axial force increases to 58 kN, approximately 48% of the yield load, and the mean cable axial force increases to 84 kN, approximately 32% of the

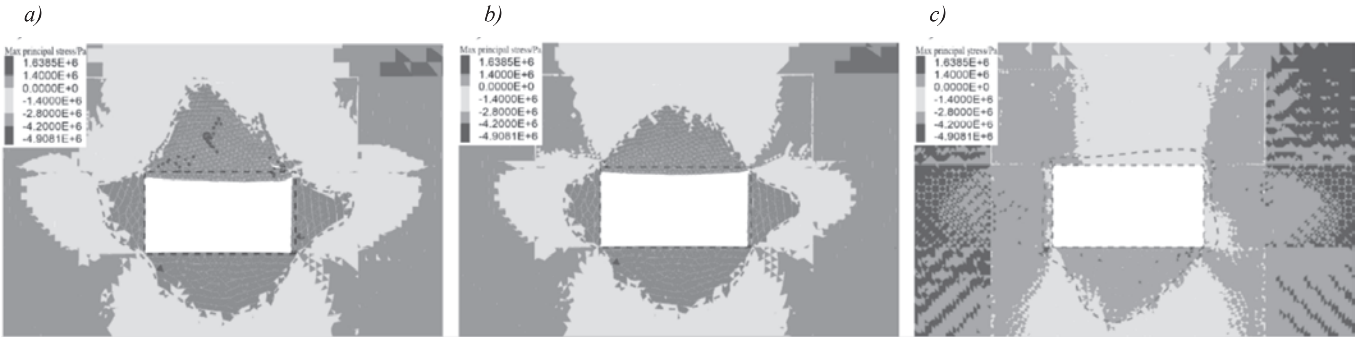


***Fig. 8.*** **Principal stress distribution under different support conditions: (a) unsupport; (b) bolt-cable support; (c) RAC system**

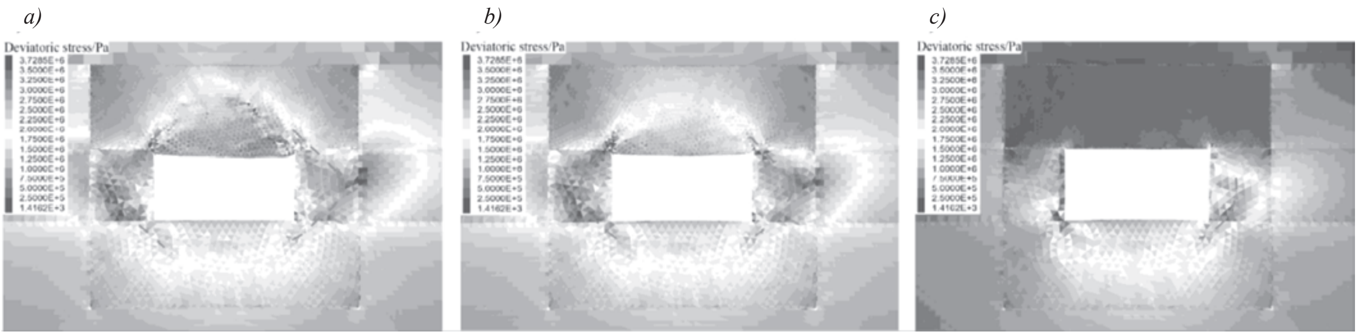


***Fig. 9.*** **Deviatoric stress distribution under different support conditions: (a) unsupport; (b) bolt-cable support; (c) RAC system**

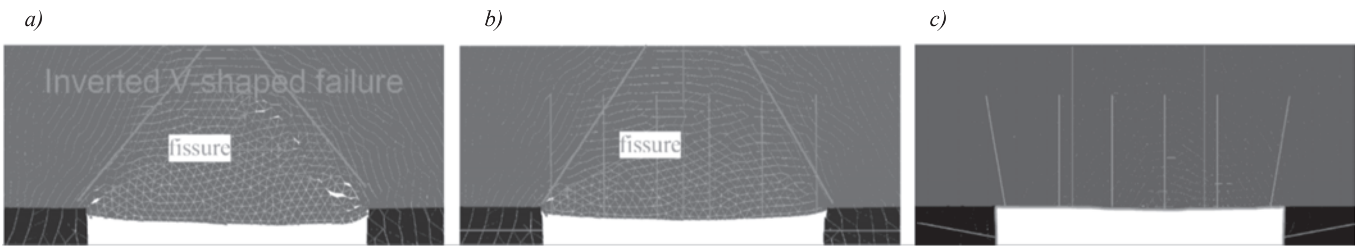


***Fig. 10.*** **Roof fracture development under different support conditions: (a) unsupport; (b) bolt-cable support; (c) RAC system**

a) b)

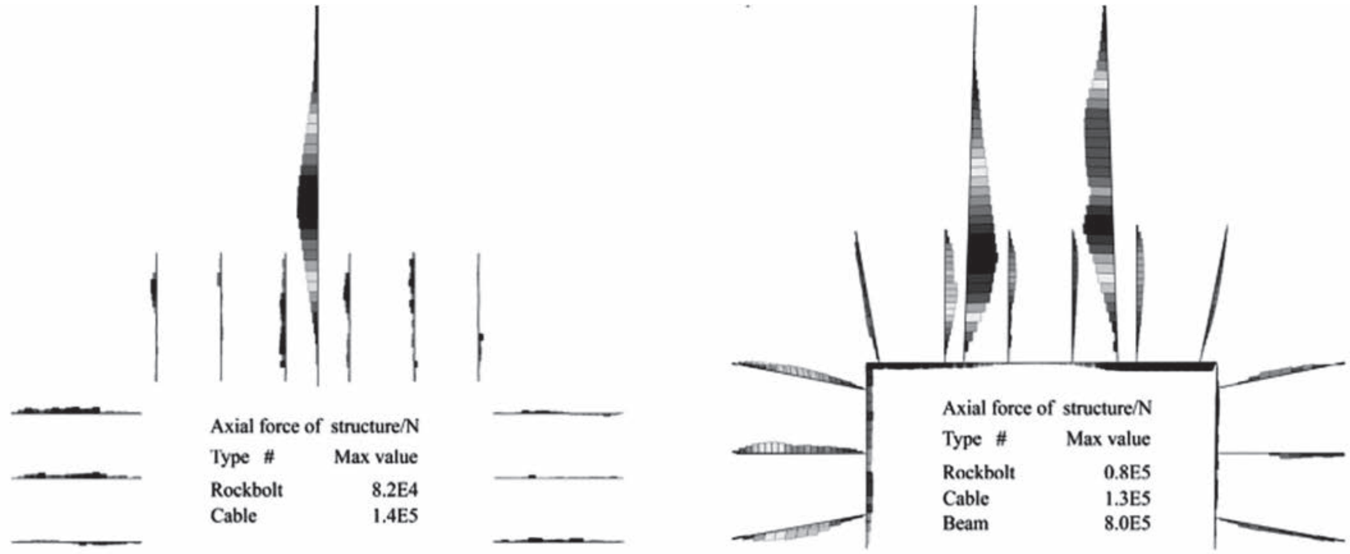


***Fig. 11.*** **Axial force distribution in support components: (a) bolt-cable support; (b) RAC system**

a) b)

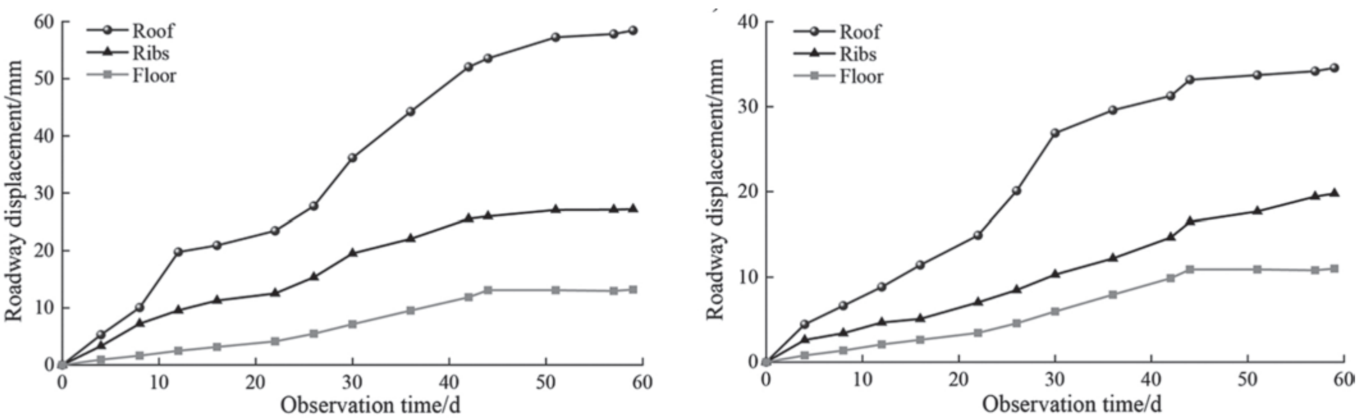


***Fig. 12.*** **Roadway convergence monitoring results: (a) central burnt rock zone; (b) burnt rock zone boundary**

a) b)

***Fig. 13.*** **Surrounding rock control performance: (a) overall cross-sectional condition; (b) condition in advance zone**

yield load. These results demonstrate that under weak and fractured surrounding rock conditions, the support components are in a good stress state and effectively play the role of anchoring and controlling the surrounding rock.

### Field Testing and Performance Evaluation

To verify the field applicability of the RAC system, convergence monitoring stations were installed following excavation of the 3202 return airway. Each station comprises four measuring points located at the midpoints of the roof, floor, and both ribs to monitor roof-to-floor and rib-to-rib convergence.

Following two months of continuous monitoring (***Fig. 12***), the results indicate that the area affected by burnt rock, cumulative roof-to-floor convergence reaches approximately 71 mm, while rib-to-rib convergence is approximately 27 mm. At 40 days postexcavation, both roof-to-floor and rib-to-rib deformations to be stable, with minimal convergence increment.

Field observations presented in ***Fig. 13*** show that the cross-section shape of the 3202 return airway under RAC system remains intact, with surrounding rock deformation controlled within acceptable engineering limits. Even in the advance zone ahead of the working face, no significant deformation is observed, and roof and rib deterioration is substantially mitigated.

Comprehensive analysis demonstrates that the RAC system proves highly effective in burnt rock affected zones. This technology enhances rock mass integrity through grouting consolidation, while blots, cables and metal shed support collectively establish a support system providing surface confinement and deep reinforcement.

**Conclusion**

1. Due to high temperature thermal alteration, the surrounding rock exhibits loose structure with extensive fracture development, resulting in significantly reduced uniaxial compressive strength and geological strength index. Both theoretical calculations and numerical simulations indicate that the loosening zone around roadways in burnt rock areas extends to 3.1~4.2 m, with rock mass stability substantially compromised.

2. The theoretical calculation results are consistent with UDEC numerical simulation and borehole observations measured data, verifying the applicability and reliability of the equivalent radius method under burnt rock conditions, which can provide theoretical reference for roadway surrounding rock stability evaluation.27 mm.

3. The proposed RAC system effectively controls the burnt rock roadway. The grouting improves rock mass integrity, while the bolts, cables and metal sheds components form a multi-level coordinated structure. Field monitoring shows that the convergence of roof-to-floor and ribs are 71 mm and respectively, the surrounding rock deformation is effectively controlled, and the long-term safe and stable support of roadway in burnt rock area is achieved.

**REFERENCES**


1. Rexiti Y., Lei H., Fan Y., et al. Characteristics and transformations of mineral phases in burnt rocks. *Coal Geol. Explor.* 2024; 52 (8): 14. https://doi.org/10.12363/issn.1001-1986.23.11.0739.
2. Jia Z.-Z., Li H.-J., Li W., et al. Study on blasting fragmentation mechanism of burnt rock in open-pit coal mine. *Sci. Rep.* 2024; 14 (1): 5034. https://doi.org/10.1038/s41598-024-55802-2.
3. Yang Y., Zhao C., Di Y., et al. Geological exploration of coal mine burnt rock and waterlogged area boundary based on transient electromagnetic and high-density electrical resistivity. *Sci. Rep.* 2024; 14 (1): 5105. https://doi.org/10.1038/s41598-024-55496-6.
4. Kang H. Seventy years development and prospects of strata control technologies for coal mine roadways in China. *Chin. J. Rock Mech. Eng.* 2021; 40 (1): 1–30. https://doi.org/10.13722/j.cnki.jrme.2020.0072.
5. Wang H., Chen M., Zhang X. Twenty years development and prospect of rapid coal mine roadway excavation in China. *J. China Coal Soc.* 2024; 49 (2): 1199–1213.
6. Kang H., Yang J., Jiang P., et al. Theory, technology and application of grouted bolting in soft rock roadways of deep coal mines. *Int J Miner Metall Mater.* 2024; 31 (7): 1463–1479. https://doi.org/10.1007/s12613-024-2906-8.
7. Wang S., Liu L., Zhu M., et al. Scientific problems and technology of the integration of “excavation-backfill-retention” of Section Coal Pillar and Mining Roadway. *J. China Coal Soc.* 2024; 49 (8): 3291–3315. https://doi.org/10.13225/j.cnki.jccs.2024.0592.
8. Xue J., Shi. L., Wang H., et al. Water abundance evaluation of a burnt rock aquifer using the AHP and entropy weight method: a case study in the Yongxin coal mine, China. *Environ. Earth Sci.* 2021; 80 (11): 417. https://doi.org/10.1007/s12665-021-09703-6.
9. Xie H., Li J., Dong Y., et al. Fast Fisher discrimination of water-rich burnt rock based on DC electrical sounding data. *Mine Water Environ.* 2021; 40 (2): 539–546. https://doi.org/10.1007/s10230-020-00747-x.
10. Zhang B., Xiao F., Jin W. Burnt coal field detection via magnetic exploration. *Environ. Earth Sci.* 2023; 82 (7): 160. https://doi.org/10.1007/s12665-023-10843-0.
11. Huang H., Sun Q., Guo C., et al. Investigating the evolution of pore space and magnetization rate of rocks under the effect of coal fire burning. *Environ. Earth Sci.* 2024; 83 (2): 81. https://doi.org/10.1007/s12665-023-11396-y.
12. Yuan Y., Liu Z., Zhu C., et al. The effect of burnt rock on inclined shaft in shallow coal seam and its control technology. *Energy Science & Engineering.* 2019; 7 (5): 1882–1895. https://doi.org/10.1002/ese3.398.
13. Kang H. Support technologies for deep and complex roadways in underground coal mines: a review. *Int J Coal Sci Technol.* 2014; 1 (3): 261–277. https://doi.org/10.1007/s40789-014-0043-0.
14. Yang T., Liu J., Luo J., et al. Study on instability mechanism of soft rock roadway and pressure-relief bolt-grouting support technology. *Sci. Rep.* 2023; 13 (1): 20667. https://doi.org/10.1038/s41598-023-47451-8.
15. Kang H., Yang J., Jiang P., et al. Theory, technology and application of grouted bolting in soft rock roadways of deep coal mines. *Int J Miner Metall Mater.* 2024; 31 (7): 1463–1479. https://doi.org/10.1007/s12613-024-2906-8.


## СВЕДЕНИЯ ОБ АВТОРЕ


***Лин Лу –***
*аспирант, Китайский университет горного дела и технологий (Пекин), 100083, г. Пекин, Китай; e-mail: linlu_cumtb@163.com*



**Информация о статье**
Поступила в редакцию: 14.11.2025
Поступила после рецензирования: 30.11.2025
Принята к публикации: 10.12.2025


## ABOUT THE AUTHOR


***Lin Lu -***
*PhD Candidate, China University of Mining and Technology (Beijing), 100083, Beijing, China; e-mail: linlu_cumtb@163.com*



**Article info**
Received: 14.11.2025
Revised: 30.11.2025
Accepted: 10.12.2025